Systematic Pharmacology and GEO Database Mining Revealed the Mechanism of XFZYD Therapy for ASCVD

Bin Liang
Zhongnan Hospital of Wuhan University
Yang Xiang
Zhongnan Hospital of Wuhan University
Xiaokang Zhang
Zhongnan Hospital of Wuhan University
Jialing Rong
Zhongnan Hospital of Wuhan University
Siying He
Zhongnan Hospital of Wuhan University
Chen Wang
Zhongnan Hospital of Wuhan University
Jing Luo
Zhongnan Hospital of Wuhan University
Fang Zheng (zhengfang@whu.edu.cn)
Zhongnan hospital of Wuhan University

Research

Keywords: Systematic pharmacology, atherosclerosis, Xuefu Zhuyu decoration, ASCVD

Posted Date: April 7th, 2020

DOI: https://doi.org/10.21203/rs.3.rs-21338/v1

Abstract

Background: Xuefu Zhuyu decoration (XFZYD), as a traditional Chinese compound recipe, has been used to treat atherosclerosis cardiovascular disease (ASCVD) for thousands of years in China, but its effective compounds and underlying treatment molecular mechanism remains promiscuous, which severely limits its clinical application.

Methods : The effective components and its targets of XFZYD were predicted and screened based on the TCMSP database. The candidate therapeutic targets of ASCVD were screened by Pharmacogenomics Knowledgebase (PharmGKB) and Comparative Toxicogenomics Database (CTD). Kyoto Encyclopedia of Genes and Genomes (KEGG) pathway analyses for target proteins were performed using DAVID database. Subsequently, protein-protein interaction (PPI) analyses were conducted using the STRING database. Differentially expressed genes in GSE71226 were identified using GEO2R. Finally, molecular docking was performed by Schrodinger software.

Results: A total of 108 effective compounds and 137 candidate therapeutic targets were screened. Analyzing the relationships among effective compounds, candidate therapeutic targets, and signaling pathways, the therapy mechanism of XFZYD for ASCVD were mainly reflected in the protection of vascular endothelium, anti-inflammatory, antioxidant stress, etc. Moreover, the expression profile in GSE71226 supported our findings, while molecular simulation docking results also demonstrated the reliability of the predicted results.

Conclusions: This study demonstrates the therapeutic potential of XFZYD for the treatment of ASCVD based on systemic pharmacology, which could provide a guiding principle for its clinical application as well as valuable insights for further drug discovery. Key words: Systematic pharmacology; atherosclerosis; Xuefu Zhuyu decoration; ASCVD

1. Background

Atherosclerosis cardiovascular disease (ASCVD) was a systemic disease based on atherosclerosis, becoming a leading killer worldwide due to the high morbidity and mortality(1). Atherosclerosis is a pathological status characterized by fibrogenesis, chronic inflammation, lipid accumulation and vascular wall immunity disorders (2, 3). As atherosclerotic plaques develop into advanced stages, brittle plaques tend to rupture(4), leading to acute cardiovascular events such as ischemic stroke and myocardial infarction.

At present, clinical medications ideas for ASCVD mainly focus on correcting of atherogenic dyslipidemia and platelet aggregation. The clinical efficacy of statins and aspirin have been well established(5, 6). Although current atherosclerosis medications can partially relieve the symptoms of ASCVD patients, gastrointestinal reactions or liver and kidney damage etc. were occur constantly, due to individual differences, adverse effects of medicine or usage without doctor's prescription, which greatly disturbs the therapeutic efficacy.

Traditional Chinese Medicine (TCM) plays an important role in the adjuvant treatment of ASCVD(7). Compared with CMM of simple prescription, TCM compound recipe has the characteristics of multi-component, multi-target and multi-pathway interaction. Xuefu Zhuyu Decoration (XFZYD), a famous herbal remedy, has been used to relieve symptoms in patients with ASCVD for thousand years in China with few adverse events(8). XFZYD was composed of 11 herbs: Radix rehmanniae, Angelica sinensis, Rhizoma Chuanxiong, Carthamus tinctorius, Radix paeoniae rubra, Fructus Aurantii, Bupleunum, Platycodon grandiflorum, Achyranthes bidentata, Licorice, Semen Pruni Persicae. The formula has been proven reliable and effective for curing ASCVD(8, 9) and its risk factors hyperlipidemia(10) and hypertension(11).

Experimental studies have shown that XFZYD could control inflammatory response(12, 13), increase coronary blood flow, improve the cardiac microcirculation, accommodate blood lipids(10), and prevent platelet aggregation, maintaining vessel growth in physiological or repair range to avoid angiogenesis in the atheromatous plaque(14).

However, due to the complexity of components of XFZYD, it is difficult to systematically explain the molecular therapy mechanism of XFZYD using conventional methods. Network pharmacology provides a new idea for fundamental studying the multi-targeted mechanism for multiple ingredients in this prescription(15). In the present study, through exploration of the complex network of XFZYD-therapeutic targets-biological processes-pathways, the therapy mechanism of XFZYD for atherosclerosis was elaborated from the perspective of multi-component, multi-target and multi-pathway.

2. Methods

2.1. Identification of effective compounds of XFZYD

The effective components in XFZYD were identified from Traditional Chinese Medicine System Pharmacology (TCMSP, http://lsp.nwu.edu.cn/browse.php) database. The database provides comprehensive information about ingredients in herbs including chemical structure, oral bioavailability (OB), half-life (HL), drug likeness (DL), drug targets, etc. The pharmacokinetic properties including absorption, distribution, metabolism, and excretion (ADME) are important contributors for bioactivities of drugs. In this study, three ADME-related parameters including oral bioavailability (OB) ≥ 30%, half-life (HL) ≥ 4, and drug likeness (DL) ≥ 0.18 were employed to identify the potential effective compounds in XFZYD. As recommended by TCMSP, the compounds with OB ≥ 30% and HL ≥ 4 have good absorption and slow metabolism after oral administration, while the compounds with DL ≥ 0.18 were chemically suitable for drug development.

2.2. Prediction of compound-related targets

The compound-related targets were predicted depending on chemical similarities and pharmacophore models via TCMSP databases. TCMSP compound data were obtained from databases such as

DrugBank, HIT, TTD, PharmGKB, etc. All the targets obtained above were standardized as gene names and UniProt IDs by searching from UniprotKB database with “Homo sapiens” species.

2.3. Identification of ASCVD-related therapeutic targets

These ASCVD-related therapeutic targets were mined from two databases including Pharmacogenomics Knowledgebase (PharmGKB) and Comparative Toxicogenomics Database (CTD). The key words were “atherosclerosis” “coronary heart disease” “angina” “acute coronary syndrome” “stroke” “transient ischemic attacks” and “peripheral arterial disease”. All the targets in PharmGKB and the top 200 targets in CTD based on inference score were selected. All the targets obtained above were standardized as gene names and UniProt IDs by searching from UniprotKB database with “Homo sapiens” species.

2.4. Network construction and topological analysis

The compound-target network of XFZYD were constructed by Cytoscape v3.7.1 software which was a tool for analysis and visualization of the biological network(16). The topological analysis was performed by the Network Analyzer module of Cytoscape software. According to the topology of network, degree centrality (DC), betweenness centrality (BC) and closeness centrality (CC) are the most important parameters for measuring the criticality of a node in the network, as well as the important index for new drug discovery and target prediction.

2.5. Protein-Protein Interaction (PPI) network construction and analysis

The PPI network was beneficial to explore the interaction of various proteins in complex diseases. The identified therapeutic targets were uploaded to the STRING database v11.0 (17) to obtain the protein-protein interaction information, including the physical and functional associations. Protein interactions with a confidence score of 0.9 or higher were obtained. The PPI network was visualized by Cytoscape v3.7.1(16). Network Analyzer was utilized for calculating the network topology parameters, in which the network was treated as undirected.

2.6. KEGG pathway enrichment analysis

The KEGG pathway enrichment analysis were carried out using DAVID database, which is an online biological knowledgebase and an analytic tool to extract biological information about gene functional classification, functional annotation, and enriched pathways(18). KEGG pathways with P value < 0.05 were considered to have significance.

2.7. GEO database validation

Peripheral blood RNA expression profiles of 3 atherosclerosis patients and 3 controls were obtained from GSE71226, the differentially expressed genes (DEGs) in GSE71226 were identified using GEO2R (https://www.ncbi.nlm.nih.gov/geo/geo2r/), $p < 0.05$ and $|\log FC| \geq 1.5$ were the screening criteria.

2.8. Binding capacity between effective compounds and key targets by molecular docking

The X-ray crystal structures of the candidate therapeutic targets were taken from the RCSB PDB database, and all 3D structures of these components were obtained from the PubChem database. Molecular docking was performed by Schrodinger software. The compounds and target proteins were input and pretreated to perform the molecular docking command, and finally the docking score was obtained. The magnitude of the absolute value of docking score is proportional to the strength of bonding.

3. Results

3.1. Effective components of XFZYD and targets

A total of 129 compounds and 256 target proteins in 11 kinds of herbs were identified in XFZYD through TCMSP database with the criteria of OB ≥ 30%, HL ≥ 4 and DL ≥ 0.18 (Table S1).

3.2. ASCVD-related targets

ASCVD-related therapeutic targets were retrieved in two databases, including 73 in PharmGKB and 582 in CTD. After removing the repeated targets, a total of 620 ASCVD-related therapeutic targets were identified (Table S2), 137 of which were overlapped with targets of XFZYD (Fig. 1).

3.3. Compound-Target network of XFZYD for the treatment of ASCVD

The compound-targets network was constructed to elaborate the multiplex interplay between compounds and their related targets of XFZYD at a systematic perspective. The compound-target network consists of 245 nodes (108 active components and 137 candidate therapeutic targets) and 945 edges (Fig. 2). The compound quercetin has 90 targets, suggesting that it may be critical in the treatment of atherosclerosis (Table 1). Topological analysis was adopted to determine the core targets and compounds of XFZYD in the treatment of ASCVD with the screening criteria “DC ≥ 3, BC ≥ 0.000348 and CC ≥ 0.3754”. The topological network consists of 87 nodes (65 active components and 22 component targets) and 447 edges (Fig. 3). From this, it can be inferred that these high-degree compounds are likely to be the core pharmacodynamic substances in the XFZYD. Besides, the compound-targets network illustrated the multi-component, multi-target characteristics of XFZYD.

Table 1

The characteristics of effective compounds in XFZYD

Mol ID	compounds	OB (%)	DL	HL	herb	Target Number
MOL000006	luteolin	36.16	0.25	15.94	Carthamus tinctorius Platycodon grandiflorum	34
MOL000098	quercetin	46.43	0.28	14.4	Bupleunum Carthamus tinctorius Achyranthes bidentata Licorice	83
MOL000173	wogonin	30.68	0.23	17.75	Achyranthes bidentata	22
MOL000239	Jaranol	50.83	0.29	15.5	Licorice	4
MOL000296	hederagenin	36.91	0.75	5.35	Semen Pruni Persicae	2
MOL000354	isorhamnetin	49.6	0.31	14.34	Bupleunum, Licorice	12
MOL000358	beta-sitosterol	36.91	0.75	5.36	Radix paeoniae rubra Angelica sinensis Carthamus tinctorius Achyranthes bidentata Semen Pruni Persicae Fructus Aurantii	10
MOL000392	formononetin	69.67	0.21	17.04	Licorice	11
MOL000417	Calycosin	47.75	0.24	17.1	Licorice	9
MOL000422	kaempferol	41.88	0.24	14.74	Bupleunum Licorice Carthamus tinctorius Achyranthes bidentata	30
MOL000433	FA	68.96	0.71	24.81	Rhizoma Chuanxiong	2

Mol ID	compounds	OB (%)	DL	HL	herb	Target Number
MOL000449	Stigmasterol	43.83	0.76	5.57	Bupleunum Radix paeoniae rubra Angelica sinensis Radix rehmanniae Carthamus tinctorius Achyranthes bidentata	3
MOL000493	campesterol	37.58	0.71	4.71	Semen Pruni Persicae	2
MOL000497	licochalcone a	40.79	0.29	16.2	Licorice	16
MOL001323	Sitosterol alpha1	43.28	0.78	5.64	Semen Pruni Persicae	1
MOL001328	2,3-didehydro GA70	63.29	0.5	7.62	Semen Pruni Persicae	2
MOL001329	2,3-didehydro GA77	88.08	0.53	7.6	Semen Pruni Persicae	1
MOL001340	GA120	84.85	0.45	8.4	Semen Pruni Persicae	1
MOL001352	GA54	64.21	0.53	10.19	Semen Pruni Persicae	1
MOL001355	GA63	65.54	0.54	9.85	Semen Pruni Persicae	1
MOL001358	gibberellin 7	73.8	0.5	9.79	Semen Pruni Persicae	1
MOL001361	GA87	68.85	0.57	8.76	Semen Pruni Persicae	1
MOL001368	3-O-p-coumaroylquinic acid	37.63	0.29	5.15	Semen Pruni Persicae	2
MOL001454	berberine	36.86	0.78	6.57	Achyranthes bidentata	4
MOL001458	coptisine	30.67	0.86	9.33	Achyranthes bidentata	4
MOL001484	Inermine	75.18	0.54	11.72	Licorice	2

Mol ID	compounds	OB (%)	DL	HL	herb	Target Number
MOL001494	Mandenol	42	0.19	5.39	Rhizoma Chuanxiong	2
MOL001645	Linoleyl acetate	42.1	0.2	7.48	Bupleunum	2
MOL001689	acacetin	34.97	0.24	17.25	Platycodon grandiflorum	12
MOL001792	DFV	32.76	0.18	17.89	Licorice	3
MOL001924	paeoniflorin	53.87	0.79	13.88	Radix paeoniae rubra	2
MOL002135	3,5,6,7-tetramethoxy -2-(3,4,5-trimethoxyphenyl) chromone	40.6	0.51	4.39	Rhizoma Chuanxiong	10
MOL002140	Perlolyrine	65.95	0.27	12.62	Rhizoma Chuanxiong	1
MOL002157	wallichilide	42.31	0.71	6.85	Rhizoma Chuanxiong	2
MOL002311	Glycyrol	90.78	0.67	9.85	Licorice	8
MOL002341	Hesperetin	70.31	0.27	15.78	Fructus Aurantii	2
MOL002565	Medicarpin	49.22	0.34	8.46	Licorice	6
MOL002695	lignan	43.32	0.65	14.88	Carthamus tinctorius	2
MOL002712	6-Hydroxykaempferol	62.13	0.27	14.29	Carthamus tinctorius	4
MOL002714	baicalein	33.52	0.21	16.25	Achyranthes bidentata Carthamus tinctorius Radix paeoniae rubra	18
MOL002721	quercetagetin	45.01	0.31	13.82	Carthamus tinctorius	2
MOL002773	beta-carotene	37.18	0.58	4.36	Carthamus tinctorius	20
MOL002897	epiberberine	43.09	0.78	6.1	Achyranthes bidentata	3

Mol ID	compounds	OB (%)	DL	HL	herb	Target Number
MOL003656	Lupiwighteone	51.64	0.37	15.63	Licorice	8
MOL003847	Inophyllum E	38.81	0.85	15.51	Achyranthes bidentata	4
MOL003896	7-Methoxy-2-methyl isoflavone	42.56	0.2	16.89	Licorice	9
MOL004328	naringenin	59.29	0.21	16.98	Licorice Fructus Aurantii	22
MOL004580	cis-Dihydroquercetin	66.44	0.27	14.51	Platycodon grandiflorum	2
MOL004598	3,5,6,7-tetramethoxy-2-(3,4,5-trimethoxyphenyl) chromone	31.97	0.59	15.54	Bupleunum	2
MOL004609	Areapillin	48.96	0.41	16.52	Bupleunum	2
MOL004805	(2S)-2-[4-hydroxy-3-(3-methylbut-2-enyl)phenyl] -8,8-dimethyl-2,3-dihydropyrano[2,3-f]chromen -4-one	31.79	0.72	14.82	Licorice	6
MOL004806	euchrenone	30.29	0.57	15.89	Licorice	3
MOL004808	glyasperin B	65.22	0.44	16.1	Licorice	8
MOL004810	glyasperin F	75.84	0.54	15.64	Licorice	9
MOL004814	Isotrifoliol	31.94	0.42	7.91	Licorice	7
MOL004815	(E)-1-(2,4-dihydroxyphenyl) -3-(2,2-dimethylchromen-6-yl) prop-2-en-1-one	39.62	0.35	16.16	Licorice	9
MOL004824	(2S)-6-(2,4-dihydroxyphenyl) -2-(2-hydroxypropan-2-yl)-4 -methoxy-2,3-dihydrofuro [3,2-g]chromen-7-one	60.25	0.63	4.31	Licorice	9
MOL004827	Semilicoisoflavone B	48.78	0.55	17.02	Licorice	6
MOL004828	Glepidotin A	44.72	0.35	16.09	Licorice	10
MOL004835	Glypallichalcone	61.6	0.19	17.01	Licorice	9
MOL004838	8-(6-hydroxy-2-benzofuranyl) -2,2-dimethyl-5-chromenol	58.44	0.38	8.71	Licorice	3
MOL004841	Licochalcone B	76.76	0.19	17.02	Licorice	9

Mol ID	compounds	OB (%)	DL	HL	herb	Target Number
MOL004848	licochalcone G	49.25	0.32	15.75	Licorice	9
MOL004855	Licoricone	63.58	0.47	16.37	Licorice	5
MOL004856	Gancaonin A	51.08	0.4	16.82	Licorice	6
MOL004857	Gancaonin B	48.79	0.45	16.49	Licorice	7
MOL004863	3-(3,4-dihydroxyphenyl)-5,7-dihydroxy-8-(3-methylbut-2-enyl) chromone	66.37	0.41	15.81	Licorice	8
MOL004864	5,7-dihydroxy-3-(4-methoxyphenyl) -8-(3-methylbut-2-enyl)chromone	30.49	0.41	14.99	Licorice	8
MOL004866	2-(3,4-dihydroxyphenyl)-5,7-dihydroxy-6-(3-methylbut-2-enyl) chromone	44.15	0.41	16.77	Licorice	4
MOL004882	Licocoumarone	33.21	0.36	9.66	Licorice	4
MOL004883	Licoisoflavone	41.61	0.42	16.09	Licorice	8
MOL004884	Licoisoflavone B	38.93	0.55	15.73	Licorice	7
MOL004885	licoisoflavanone	52.47	0.54	15.67	Licorice	8
MOL004891	shinpterocarpin	80.3	0.73	6.5	Licorice	9
MOL004898	(E)-3-[3,4-dihydroxy-5-(3-methylbut-2-enyl)phenyl] -1-(2,4-dihydroxyphenyl)prop -2-en-1-one	46.27	0.31	15.24	Licorice	7
MOL004903	liquiritin	65.69	0.74	17.96	Licorice	3
MOL004907	Glyzaglabrin	61.07	0.35	21.2	Licorice	9
MOL004910	Glabranin	52.9	0.31	16.24	Licorice	4
MOL004912	Glabrone	52.51	0.5	16.09	Licorice	9
MOL004913	1,3-dihydroxy-9-methoxy-6-benzofurano[3,2-c]chromenone	48.14	0.43	8.87	Licorice	6
MOL004914	1,3-dihydroxy-8,9-dimethoxy-6-benzofurano[3,2-c]chromenone	62.9	0.53	9.32	Licorice	5
MOL004915	Eurycarpin A	43.28	0.37	17.1	Licorice	8

Mol ID	compounds	OB (%)	DL	HL	herb	Target Number
MOL004924	(-)-Medicocarpin	40.99	0.95	13.2	Licorice	1
MOL004935	Sigmoidin-B	34.88	0.41	14.49	Licorice	3
MOL004941	(2R)-7-hydroxy-2-(4-hydroxyphenyl) chroman-4-one	71.12	0.18	18.09	Licorice	3
MOL004945	(2S)-7-hydroxy-2-(4-hydroxyphenyl) -8-(3-methylbut-2-enyl)chroman-4-one	36.57	0.32	17.95	Licorice	4
MOL004948	Isoglycyrol	44.7	0.84	6.69	Licorice	4
MOL004949	Isolicoflavonol	45.17	0.42	15.55	Licorice	7
MOL004957	HMO	38.37	0.21	16.56	Licorice	9
MOL004959	1-Methoxyphaseollidin	69.98	0.64	9.53	Licorice	10
MOL004961	Quercetin der.	46.45	0.33	16.61	Licorice	8
MOL004988	Kanzonol F	32.47	0.89	9.98	Licorice	2
MOL004989	6-prenylated eriodictyol	39.22	0.41	16.52	Licorice	3
MOL004991	7-Acetoxy-2-methylisoflavone	38.92	0.26	17.49	Licorice	8
MOL004993	8-prenylated eriodictyol	53.79	0.4	15.7	Licorice	2
MOL005000	Gancaonin G	60.44	0.39	16.13	Licorice	7
MOL005001	Gancaonin H	50.1	0.78	16.64	Licorice	4
MOL005003	Licoagrocarpin	58.81	0.58	9.45	Licorice	9
MOL005007	Glyasperins M	72.67	0.59	15.57	Licorice	9
MOL005008	Glycyrrhiza flavonol A	41.28	0.6	13.71	Licorice	6
MOL005012	Licoagroisoflavone	57.28	0.49	19.64	Licorice	8
MOL005016	Odoratin	49.95	0.3	16.35	Licorice	9
MOL005017	Phaseol	78.77	0.58	9.64	Licorice	8
MOL005018	Xambioona	54.85	0.87	14.5	Licorice	3
MOL005828	nobiletin	61.67	0.52	16.2	Fructus Aurantii	15

Mol ID	compounds	OB (%)	DL	HL	herb	Target Number
MOL006992	(2R,3R)-4-methoxyl-distylin	59.98	0.3	15.08	Radix paeoniae rubra	4
MOL013187	Cubebin	57.13	0.64	12.4	Bupleunum	2
MOL013381	Marmin	38.23	0.31	4.68	Fructus Aurantii	1

3.4. PPI network construction and topology analysis

In order to elucidate the systemic and pharmacological therapy mechanism of XFZYD for ASCVD, PPI network with 137 candidate therapeutic targets were constructed and visualized. Totally, 137 nodes and 598 edges were obtained in this network (Fig. 4A). Then, topological analysis was adopted to determine the core targets of XFZYD in the treatment of ASCVD with the screening criteria “DC ≥ 14, BC ≥ 0.00382 and CC ≥ 0.3598”. Finally, we identified 27 core targets of XFZYD (Fig. 4B), indicating that they might serve as vital targets of XFZYD in treating ASCVD.

3.5. KEGG enrichment analysis

KEGG pathway enrichment analysis was performed to elucidate 137 candidate therapeutic targets of XFZYD for ASCVD. The representative top 20 pathways based on the number of enriched genes as well as P value were shown in Fig. 5. These key targets were closely related to TNF signaling pathway, PI3K-Akt signaling pathway, VEGF signaling pathway, Toll-like receptor signaling pathway, etc., participating in the process of atherosclerotic plaque formation, such as oxidative stress, inflammatory response, angiogenesis etc.

3.6. Clinical validation based on GEO database

In accordance with the analysis of GSE71226 microarray data of atherosclerosis, 673 differentially expressed genes were identified, among which 133 were up-regulated and 540 were down-regulated in the atherosclerosis group (Table S3). There were 6 targets in the intersection with 137 candidate therapeutic targets of XFZYD, which included up-regulated PTGS2, MMP9 and BCL2L1 and downregulated JUN, VEGFA and CXCL2 in atherosclerosis group (Table 2). It was indicated that the prediction of candidate therapeutic targets of XFZYD for ASCVD was relatively reliable.

Table 2

DEGs that overlapped with potential therapeutic targets of XFZYD

Group	Gene symbol	Gene title	Pvalue	logFC
up-regulated genes	BCL2L1	BCL2 like 1	0.0163396	2.38
	MMP9	matrix metallopeptidase 9	0.0187166	2.27
	PTGS2	prostaglandin-endoperoxide synthase 2	0.0374968	1.75
down-regulated genes	CXCL2	C-X-C motif chemokine ligand 2	0.00806	-1.59
	JUN	Jun proto-oncogene, AP-1 transcription factor subunit	0.0008752	-1.99
	VEGFA	vascular endothelial growth factor A	0.0011307	-1.69

Table 3: The docking score of XFZYD on atherosclerosis

Target	PDB ID	MOL ID	Docking score
BCL2L1	3SP7	MOL000006	-6.145
BCL2L1	3SP7	MOL000098	-5.739
CXCL2	5OB5	MOL000098	-7.022
IL-6	5FUC	MOL000006	-6.559
IL-6	5FUC	MOL000098	-6.587
IL-6	5FUC	MOL000173	-5.028
IL-6	5FUC	MOL001924	-3.395
JUN	5T01	MOL000006	-5.814
JUN	5T01	MOL000098	-5.495
JUN	5T01	MOL000173	-4.631
JUN	5T01	MOL000358	-1.212
JUN	5T01	MOL000392	-4.504
JUN	5T01	MOL000422	-4.760
JUN	5T01	MOL002773	-1.504
JUN	5T01	MOL005828	-2.709
MAPK1	6RQ4	MOL000006	-6.292
MAPK1	6RQ4	MOL000098	-5.611

Group	Gene symbol	Gene title	Pvalue	logFC
MAPK1	6RQ4	MOL000497	-5.500	
MAPK1	6RQ4	MOL004328	-5.543	
MAPK14	6SFI	MOL000173	-7.106	
MAPK14	6SFI	MOL000354	-7.148	
MAPK14	6SFI	MOL000392	-7.289	
MAPK14	6SFI	MOL000417	-6.768	
MAPK14	6SFI	MOL000497	-7.545	
MAPK14	6SFI	MOL002311	-8.550	
MAPK14	6SFI	MOL003656	-6.756	
MAPK14	6SFI	MOL004805	-8.946	
MAPK14	6SFI	MOL004810	-6.284	
MAPK14	6SFI	MOL004814	-7.366	
MAPK14	6SFI	MOL004815	-7.033	
MAPK14	6SFI	MOL004824	-8.328	
MAPK14	6SFI	MOL004835	-7.692	
MAPK14	6SFI	MOL004841	-7.093	
MAPK14	6SFI	MOL004848	-7.745	
MAPK14	6SFI	MOL004891	-5.477	
MAPK14	6SFI	MOL004898	-8.043	
MAPK14	6SFI	MOL004907	-7.248	
MAPK14	6SFI	MOL004912	-7.459	
MAPK14	6SFI	MOL004915	-8.093	
MAPK14	6SFI	MOL004991	-6.097	
MAPK14	6SFI	MOL005000	-7.018	
MAPK14	6SFI	MOL005012	-7.403	
MAPK14	6SFI	MOL005016	-7.159	
MAPK14	6SFI	MOL005017	-7.018	

Group	Gene symbol	Gene title	Pvalue	logFC
MAPK3	6GES	MOL004328	-5.671	
MMP9	6ESM	MOL000006	-5.700	
MMP9	6ESM	MOL000098	-6.312	
MMP9	6ESM	MOL002714	-4.905	
MMP9	6ESM	MOL005828	-2.798	
PTGS2	5F19	MOL000006	-7.716	
PTGS2	5F19	MOL000098	-7.902	
PTGS2	5F19	MOL000173	-7.521	
PTGS2	5F19	MOL000239	-7.429	
PTGS2	5F19	MOL000354	-7.474	
PTGS2	5F19	MOL000358	-7.453	
PTGS2	5F19	MOL000392	-7.170	
PTGS2	5F19	MOL000417	-7.579	
PTGS2	5F19	MOL000422	-7.507	
PTGS2	5F19	MOL000449	-7.565	
PTGS2	5F19	MOL000493	-7.117	
PTGS2	5F19	MOL000497	-7.415	
PTGS2	5F19	MOL001323	-6.811	
PTGS2	5F19	MOL001340	-5.115	
PTGS2	5F19	MOL001352	-5.830	
PTGS2	5F19	MOL001355	-6.828	
PTGS2	5F19	MOL001361	-5.160	
PTGS2	5F19	MOL001454	-7.544	
PTGS2	5F19	MOL001458	-7.601	
PTGS2	5F19	MOL001484	-6.701	
PTGS2	5F19	MOL001494	-5.521	
PTGS2	5F19	MOL001645	-4.539	

Group	Gene symbol	Gene title	Pvalue	logFC
PTGS2	5F19	MOL001689	-7.464	
PTGS2	5F19	MOL001792	-6.831	
PTGS2	5F19	MOL002135	-5.624	
PTGS2	5F19	MOL002140	-6.557	
PTGS2	5F19	MOL002157	-4.973	
PTGS2	5F19	MOL002311	-8.494	
PTGS2	5F19	MOL002341	-7.550	
PTGS2	5F19	MOL002565	-6.253	
PTGS2	5F19	MOL002712	-7.368	
PTGS2	5F19	MOL002714	-6.836	
PTGS2	5F19	MOL002721	-7.576	
PTGS2	5F19	MOL002773	-7.722	
PTGS2	5F19	MOL002897	-6.881	
PTGS2	5F19	MOL003656	-8.177	
PTGS2	5F19	MOL003847	-6.824	
PTGS2	5F19	MOL004328	-7.913	
PTGS2	5F19	MOL004580	-7.975	
PTGS2	5F19	MOL004805	-7.974	
PTGS2	5F19	MOL004808	-7.335	
PTGS2	5F19	MOL004810	-8.041	
PTGS2	5F19	MOL004814	-7.258	
PTGS2	5F19	MOL004815	-8.037	
PTGS2	5F19	MOL004824	-8.075	
PTGS2	5F19	MOL004827	-7.706	
PTGS2	5F19	MOL004828	-6.869	
PTGS2	5F19	MOL004835	-6.103	
PTGS2	5F19	MOL004841	-6.607	

Group	Gene symbol	Gene title	Pvalue	logFC
PTGS2	5F19	MOL004848	-7.360	
PTGS2	5F19	MOL004855	-7.877	
PTGS2	5F19	MOL004856	-8.120	
PTGS2	5F19	MOL004857	-9.344	
PTGS2	5F19	MOL004884	-8.878	
PTGS2	5F19	MOL004885	-7.210	
PTGS2	5F19	MOL004891	-7.345	
PTGS2	5F19	MOL004898	-7.917	
PTGS2	5F19	MOL004903	-7.345	
PTGS2	5F19	MOL004907	-7.725	
PTGS2	5F19	MOL004910	-7.343	
PTGS2	5F19	MOL004912	-7.642	
PTGS2	5F19	MOL004915	-7.446	
PTGS2	5F19	MOL004924	-4.804	
PTGS2	5F19	MOL004935	-7.894	
PTGS2	5F19	MOL004948	-8.152	
PTGS2	5F19	MOL004949	-8.086	
PTGS2	5F19	MOL004959	-7.705	
PTGS2	5F19	MOL004988	-5.016	
PTGS2	5F19	MOL004991	-7.575	
PTGS2	5F19	MOL005000	-8.757	
PTGS2	5F19	MOL005001	-7.045	
PTGS2	5F19	MOL005003	-6.510	
PTGS2	5F19	MOL005008	-8.224	
PTGS2	5F19	MOL005012	-7.780	
PTGS2	5F19	MOL005016	-7.258	
PTGS2	5F19	MOL005017	-7.847	

Group	Gene symbol	Gene title	Pvalue	logFC
PTGS2	5F19	MOL005018	-6.991	
PTGS2	5F19	MOL005828	-7.270	
PTGS2	5F19	MOL013187	-7.200	
PTGS2	5F19	MOL013381	-6.758	
RELA	3QXY	MOL000006	-5.254	
RELA	3QXY	MOL000098	-6.271	
RELA	3QXY	MOL000173	-4.963	
RELA	3QXY	MOL000354	-5.728	
RELA	3QXY	MOL000422	-5.817	
RELA	3QXY	MOL000497	-5.488	
RELA	3QXY	MOL001689	-5.400	
RELA	3QXY	MOL002714	-5.166	
RELA	3QXY	MOL004328	-5.864	
STAT3	6NJS	MOL000497	-4.473	
VEGFA	4KZN	MOL000006	-5.593	
VEGFA	4KZN	MOL000098	-5.617	
VEGFA	4KZN	MOL002714	-4.422	
HSP90AA1	6U99	MOL000006	-5.964	
HSP90AA1	6U99	MOL000098	-5.850	
HSP90AA1	6U99	MOL004915	-5.759	
HSP90AA1	6U99	MOL004883	-5.597	
HSP90AA1	6U99	MOL004949	-5.482	
HSP90AA1	6U99	MOL000422	-5.394	
HSP90AA1	6U99	MOL002721	-5.246	
HSP90AA1	6U99	MOL001368	-5.198	
HSP90AA1	6U99	MOL004580	-5.219	
HSP90AA1	6U99	MOL004907	-5.136	

Group	Gene symbol	Gene title	Pvalue	logFC
HSP90AA1	6U99	MOL001792	-5.079	
HSP90AA1	6U99	MOL004808	-5.037	
HSP90AA1	6U99	MOL004935	-5.047	
HSP90AA1	6U99	MOL004328	-4.921	
HSP90AA1	6U99	MOL004882	-4.809	
HSP90AA1	6U99	MOL000239	-4.769	
HSP90AA1	6U99	MOL005017	-4.747	
HSP90AA1	6U99	MOL002714	-4.738	
HSP90AA1	6U99	MOL000417	-4.620	
HSP90AA1	6U99	MOL002565	-4.602	
HSP90AA1	6U99	MOL003656	-4.460	
HSP90AA1	6U99	MOL002712	-4.471	
HSP90AA1	6U99	MOL005000	-4.425	
HSP90AA1	6U99	MOL001689	-4.392	
HSP90AA1	6U99	MOL001689	-4.392	
HSP90AA1	6U99	MOL004810	-4.409	
HSP90AA1	6U99	MOL004841	-4.422	
HSP90AA1	6U99	MOL004827	-4.344	
HSP90AA1	6U99	MOL004959	-4.316	
HSP90AA1	6U99	MOL000173	-4.329	
HSP90AA1	6U99	MOL000392	-4.282	
HSP90AA1	6U99	MOL004835	-4.204	
HSP90AA1	6U99	MOL001484	-4.176	
HSP90AA1	6U99	MOL005003	-4.154	
HSP90AA1	6U99	MOL013187	-4.065	
HSP90AA1	6U99	MOL000497	-4.121	
HSP90AA1	6U99	MOL004898	-4.321	

Group	Gene symbol	Gene title	Pvalue	logFC
HSP90AA1	6U99	MOL004857	-4.006	
HSP90AA1	6U99	MOL004910	-3.861	
HSP90AA1	6U99	MOL004848	-4.067	
HSP90AA1	6U99	MOL000354	-3.810	
HSP90AA1	6U99	MOL004885	-3.617	
HSP90AA1	6U99	MOL001454	-3.560	
HSP90AA1	6U99	MOL004828	-3.563	
HSP90AA1	6U99	MOL004814	-3.558	
HSP90AA1	6U99	MOL002341	-3.539	
HSP90AA1	6U99	MOL005016	-3.506	
HSP90AA1	6U99	MOL004856	-3.465	
HSP90AA1	6U99	MOL004991	-3.335	
HSP90AA1	6U99	MOL002135	-3.264	
HSP90AA1	6U99	MOL005008	-3.231	
HSP90AA1	6U99	MOL001352	-2.866	
HSP90AA1	6U99	MOL000358	-2.863	
HSP90AA1	6U99	MOL005001	-1.997	

3.7. Molecular docking

To further verify the binding capacity between active compounds and key targets, molecular docking through Schrodinger was performed. The degree ranked the top 10 target proteins of PPI topology analysis network and 6 DEGs that overlapped with candidate therapeutic targets were selected as docking objects. Since the PDB structures of FOS have no original ligands, further analysis has to pause. The docking results were listed in Table 3, where PTGS2 and Inophyllum E exhibited the tightest binding (Fig. 6). There were 9 targets that bind to the compound luteolin and 10 targets binding to the quercetin in these 13 docking targets, indicating a major role of luteolin and quercetin for XFZYD in the treatment of ASCVD.

4. Discussion

ASCVD is a kind of complex and multifactorial disease and remains the leading cause of death worldwide(19). TCM has characteristics of multi-component and multi-target, which can affect different biological processes to control symptoms and solve the fundamental problems.

In the present study, the effective compounds and candidate therapeutic targets in XFZYD for the treatment of ASCVD were 109 and 137, respectively. Moreover, 56.2% of 137 candidate therapeutic targets of XFZYD could be overlapped by at least 2 effective compounds, which demonstrated the effective compounds in XFZYD worked against ASCVD through a multitarget synergistic way. In addition, 94.44% of 108 effective compounds acted on at least 2 candidate therapeutic targets. Besides, luteolin was contained in 2 herbs (Carthamus tinctorius and Platycodon grandiflorum), quercetin was contained in 4 herbs (Bupleunum, Carthamus tinctorius, Achyranthes bidentate and Licorice), and kaempferol was contained in 4 herbs (Bupleunum, Licorice, Carthamus tinctorius and Achyranthes bidentate) acted on 35, 90 and 33 candidate therapeutic targets against ASCVD, respectively, suggesting that XFZYD is a combination of multiple herbs, multiple compounds and multiple targets in the treatment of ASCVD. Quercetin could effectively regulate the inflammatory process of atherosclerosis by attenuating TLR-NF-κB signaling pathway in vascular endothelial cells to inhibit the adhesion of leukocyte (20). Luteolin significantly reduced atherosclerosis induced by high-fat diet in ApoE mice and reduced ox-LDL-induced inflammatory response in vitro by inhibiting transcriptional activator 3 (STAT3)(21). Kaempferol could alleviates ox-LDL-induced apoptosis in HAECs by inhibiting the TLR4/NF-κB signaling pathway(22), and mediated lipid accumulation reduction and cholesterol efflux increase from THP-1-derived macrophages and inhibited the formation of ox-LDL-induced macrophage foam cell(23).

KEGG pathway analysis showed that these candidate therapeutic targets were highly correlated with atherosclerosis, mainly involving inflammatory response, oxidative stress, angiogenesis and apoptosis. It was suggested that XFZYD may influence the inflammatory response in atherosclerosis by affecting TNF signaling pathway and Toll-like receptor (TLR) signaling pathway.

As for the TNF signaling pathway, its downstream genes were mostly involved in inflammatory response, the pro-inflammatory cytokine IL-1β activates the nuclear factor-κB (NF-κB) signaling pathway(24), induces the production of various pro-inflammatory cytokines such as TNF-α and IL-6, and positively regulates the further activation of NF-κB, resulting in an inflammatory cascade amplification effect(25). Monocyte chemoattractant protein-1(MCP-1) recruited monocytes to migrate to the damaged vascular endothelium, then monocytes differentiate into macrophages, ingesting lipid particles transform into foam cells, leading to local amplification of inflammatory effect(26). Matrix metalloproteinases-9 (MMP9), the downstream product of TNF signaling pathway, is an important member of the matrix metalloproteinase family, which could promote the degradation and remodeling of extracellular matrix in the pathological state caused by inflammatory mediators, leading to the instability and rupture of atherosclerotic plaques, thrombosis and other complications(27, 28). Meanwhile, the expression of MMP9 in peripheral blood of atherosclerosis patients was significantly up-regulated compared with the control group, confirming MMP9 was a potential therapeutic target for atherosclerosis, consistent with our predicted therapeutic targets of XFZYD.

With reference to the TLRs pathway(29), it includes TLRs, the well-defined pattern recognition receptors of immune system, in the chronic inflammation and immune response in atherosclerosis(30). TLRs engagement with their ligands stimulates pro-inflammatory cytokine production and foam cell generation, mediating the occurrence and development of coronary atherosclerotic plaque by regulating inflammation and immune response(31). Activation of the TLR signaling pathway leads to the production of multiple pro-inflammatory cytokines (IL-6, TNF-α) and chemokines (IL-8, MIP2), leading to the emergence of inflammatory responses(32, 33), accelerating the pathological process of atherosclerosis.

Moreover, the accumulation of vascular smooth muscle cells (VSMCs) promotes plaque formation and development by migrating, proliferating, and secreting extracellular matrix to interact with other cellular components leading to the formation of plaques and thickening of the vascular wall, and finally a narrowing of the blood vessels(34–36). Studies have shown that the activation of the PI3K-Akt signaling pathway aggravates atherosclerotic injury in atherosclerosis mice(37), and has an inhibitory effect on the apoptosis of VSMCs(38). In view of the promotion effect of PI3K-Akt pathway on atherosclerosis and the increased expression of BCL2L1 (product of PI3K-Akt pathway), PI3K-Akt signaling pathway may be a crucial pathway to inhibit the apoptosis of VSMCs as well as accelerate the accumulation of plaque atherosclerosis, suggesting that inhibiting PI3K-Akt signaling pathway may be one of the pathways for XFZYD to treat atherosclerosis.

In addition, vascular endothelial dysfunction was the initiating factor of atherosclerosis(39). Vascular endothelial growth factor-A (VEGFA), the most specific and prominent angiogenic factor of VEGF family, has been reported to promote the proliferation and differentiation of vascular endothelial cells, promotes vascular endothelial regeneration, regulates vascular endothelial permeability(40). It was reported that endothelial production of VEGFA may elicit a protective response to vascular injury(41). In the present study, the expression of VEGFA in atherosclerosis group were significantly decreased and the VEGFA has a larger degree in PPI topological analysis of candidate therapeutic targets of XFZYD, suggesting that inhibition of VEGF signaling pathway may be a potential pathway for XFZYD to treat atherosclerosis.

However, there were still shortcomings in this research. Since the pathological development of atherosclerosis involves complex pathological processes, the mechanism predicted above of XFZYD in treating atherosclerosis still needs to be supplemented by in vivo and in vitro experiments.

5. Conclusions

In the present study, we identified effective compounds of XFZYD that could potentially antagonize atherosclerosis through drug targets prediction, gene microarray analysis and network construction with reliable methods, which hopefully could accelerate the clinical application of XFZYD to the whole world.

Abbreviations

XFZYD Xuefu Zhuyu decoration

ASCVD atherosclerosis cardiovascular disease

TCM Traditional Chinese Medicine

TCMSP Traditional Chinese Medicine System Pharmacology

OB oral bioavailability

HL half-life

DL drug likeness

ADME absorption, distribution, metabolism, and excretion

PharmGKB Pharmacogenomics Knowledgebase

CTD Comparative Toxicogenomics Database

DC degree centrality

BC betweenness centrality

CC closeness centrality

PPI Protein-Protein Interaction

DEGs differentially expressed genes

TLR Toll-like receptor

NF-κB nuclear factor-κB

MCP-1 Monocyte chemoattractant protein-1

MMP9 Matrix metalloproteinases-9

VSMCs vascular smooth muscle cells

VEGFA vascular endothelial growth factor-A

Declarations

Authors' contributions

FZ designed the experiments. BL, YX, and XZ wrote the manuscript and conducted the pharmacology information analyses. BL, JR, and SH visualized the data. CW and JL helped to do some supplement. All authors read and approved the final manuscript.

Funding

This work was supported by the Grant of National Natural Science Foundation of China (Grant Numbers.81871722).

Availability of data and materials

The datasets used and/or analysed during the current study are available from the corresponding author on reasonable request.

Ethics approval and consent to participate

Not applicable.

Consent for publication

Not applicable.

Competing interests

The authors declare that they have no competing interests.

References

1. Jee Y, Jung KJ, Lee S, Back JH, Jee SH, Cho SI. Smoking and atherosclerotic cardiovascular disease risk in young men: the Korean Life Course Health Study. BMJ Open. 2019;9(6):e024453.
2. Libby P, Buring JE, Badimon L, Hansson GK, Deanfield J, Bittencourt MS, et al. Atherosclerosis Nat Rev Dis Primers. 2019;5(1):56.
3. Marchio P, Guerra-Ojeda S, Vila JM, Aldasoro M, Victor VM, Mauricio MD. Targeting Early Atherosclerosis: A Focus on Oxidative Stress and Inflammation. Oxid Med Cell Longev. 2019;2019:8563845.
4. Badimon L, Vilahur G. Thrombosis formation on atherosclerotic lesions and plaque rupture. J Intern Med. 2014;276(6):618–32.
5. Zhang L, He S, Li Z, Gan X, Li S, Cheng X, et al. Apolipoprotein E polymorphisms contribute to statin response in Chinese ASCVD patients with dyslipidemia. Lipids Health Dis. 2019;18(1):129.
6. Mannu GS, Macartney A, Lambert JR, Bettencourt-Silva JH, Lawn M, Lyall H, et al. The clinical utility of Multiplate analyser measurement in platelet function testing following stroke and transient ischaemic attack. Eur J Haematol. 2015;94(2):138–44.
7. Ren Y, Qiao W, Fu D, Han Z, Liu W, Ye W, et al. Traditional Chinese Medicine Protects against Cytokine Production as the Potential Immunosuppressive Agents in Atherosclerosis. J Immunol Res. 2017;2017:7424307.

8. Yang X, Xiong X, Yang G, Wang J. Chinese patent medicine Xuefu Zhuyu capsule for the treatment of unstable angina pectoris: A systematic review of randomized controlled trials. Complement Ther Med. 2014;22(2):391–9.
9. Yang T, Li X, Lu Z, Han X, Zhao M. Effectiveness and safety of Xuefu Zhuyu decoction for treating coronary heart disease angina: A systematic review and meta-analysis. Med (Baltim). 2019;98(9):e14708.
10. Wang S, Qiu XJ. The efficacy of Xue Fu Zhu Yu prescription for hyperlipidemia: A meta-analysis of randomized controlled trials. Complement Ther Med. 2019;43:218–26.
11. Wang P, Xiong X, Li S. Efficacy and Safety of a Traditional Chinese Herbal Formula Xuefu Zhuyu Decoction for Hypertension: A Systematic Review and Meta-Analysis. Med (Baltim). 2015;94(42):e1850.
12. Xing Z, Xia Z, Peng W, Li J, Zhang C, Fu C, et al. Xuefu Zhuyu decoction, a traditional Chinese medicine, provides neuroprotection in a rat model of traumatic brain injury via an anti-inflammatory pathway. Sci Rep. 2016;6:20040.
13. Wang J, Yang X, Chu F, Chen J, He Q, Yao K, et al. The effects of xuefu zhuyu and shengmai on the evolution of syndromes and inflammatory markers in patients with unstable angina pectoris after percutaneous coronary intervention: a randomised controlled clinical trial. Evid Based Complement Alternat Med. 2013;2013:896467.
14. Song J, Chen WY, Wu LY, Zheng LP, Lin W, Gao D, et al. A microarray analysis of angiogenesis modulation effect of Xuefu Zhuyu Decoction on endothelial cells. Chin J Integr Med. 2012;18(7):502–6.
15. Hopkins AL. Network pharmacology. Nat Biotechnol. 2007;25(10):1110–1.
16. Shannon P, Markiel A, Ozier O, Baliga NS, Wang JT, Ramage D, et al. Cytoscape: a software environment for integrated models of biomolecular interaction networks. Genome Res. 2003;13(11):2498–504.
17. Szklarczyk D, Morris JH, Cook H, Kuhn M, Wyder S, Simonovic M, et al. The STRING database in 2017: quality-controlled protein-protein association networks, made broadly accessible. Nucleic Acids Res. 2017;45(D1):D362-D8.
18. Jiao X, Sherman BT, Huang da W, Stephens R, Baseler MW, Lane HC, et al. DAVID-WS: a stateful web service to facilitate gene/protein list analysis. Bioinformatics. 2012;28(13):1805–6.
19. Herrington W, Lacey B, Sherliker P, Armitage J, Lewington S. Epidemiology of Atherosclerosis and the Potential to Reduce the Global Burden of Atherothrombotic Disease. Circ Res. 2016;118(4):535–46.
20. Bhaskar S, Sudhakaran PR, Helen A. Quercetin attenuates atherosclerotic inflammation and adhesion molecule expression by modulating TLR-NF-kappaB signaling pathway. Cell Immunol. 2016;310:131–40.
21. Ding X, Zheng L, Yang B, Wang X, Ying Y. Luteolin Attenuates Atherosclerosis Via Modulating Signal Transducer And Activator Of Transcription 3-Mediated Inflammatory Response. Drug Des Devel Ther. 2019;13:3899–911.

22. Zhong X, Zhang L, Li Y, Li P, Li J, Cheng G. Kaempferol alleviates ox-LDL-induced apoptosis by up-regulation of miR-26a-5p via inhibiting TLR4/NF-kappaB pathway in human endothelial cells. Biomed Pharmacother. 2018;108:1783–9.
23. Li XY, Kong LX, Li J, He HX, Zhou YD. Kaempferol suppresses lipid accumulation in macrophages through the downregulation of cluster of differentiation 36 and the upregulation of scavenger receptor class B type I and ATP-binding cassette transporters A1 and G1. Int J Mol Med. 2013;31(2):331–8.
24. Ren HY, Huang GL, Liu WM, Zhang W, Liu Y, Su GQ, et al. IL-1beta induced RXRalpha overexpression through activation of NF-kappaB signaling in gastric carcinoma. Biomed Pharmacother. 2016;78:329–34.
25. Luo Y, Zheng SG. Hall of Fame among Pro-inflammatory Cytokines: Interleukin-6 Gene and Its Transcriptional Regulation Mechanisms. Front Immunol. 2016;7:604.
26. Zhang X, Mosser DM. Macrophage activation by endogenous danger signals. J Pathol. 2008;214(2):161–78.
27. Walz W, Cayabyab FS. Neutrophil Infiltration and Matrix Metalloproteinase-9 in Lacunar Infarction. Neurochem Res. 2017;42(9):2560–5.
28. Rossano R, Larocca M, Riviello L, Coniglio MG, Vandooren J, Liuzzi GM, et al. Heterogeneity of serum gelatinases MMP-2 and MMP-9 isoforms and charge variants. J Cell Mol Med. 2014;18(2):242–52.
29. Ross R. Atherosclerosis–an inflammatory disease. N Engl J Med. 1999;340(2):115–26.
30. Seneviratne AN, Monaco C. Role of inflammatory cells and toll-like receptors in atherosclerosis. Curr Vasc Pharmacol. 2015;13(2):146–60.
31. Lin J, Kakkar V, Lu X. Essential Roles of Toll-Like Receptors in Atherosclerosis. Curr Med Chem. 2016;23(5):431–54.
32. Ospelt C, Gay S. TLRs and chronic inflammation. Int J Biochem Cell Biol. 2010;42(4):495–505.
33. Joosten LA, Abdollahi-Roodsaz S, Dinarello CA, O'Neill L, Netea MG. Toll-like receptors and chronic inflammation in rheumatic diseases: new developments. Nat Rev Rheumatol. 2016;12(6):344–57.
34. Li M, Qian M, Kyler K, Xu J. Endothelial-Vascular Smooth Muscle Cells Interactions in Atherosclerosis. Front Cardiovasc Med. 2018;5:151.
35. Jager NA, Wallis de Vries BM, Hillebrands JL, Harlaar NJ, Tio RA, Slart RH, et al. Distribution of Matrix Metalloproteinases in Human Atherosclerotic Carotid Plaques and Their Production by Smooth Muscle Cells and Macrophage Subsets. Mol Imaging Biol. 2016;18(2):283–91.
36. Frismantiene A, Philippova M, Erne P, Resink TJ. Smooth muscle cell-driven vascular diseases and molecular mechanisms of VSMC plasticity. Cell Signal. 2018;52:48–64.
37. Sun G, Li Y, Ji Z. Up-regulation of MIAT aggravates the atherosclerotic damage in atherosclerosis mice through the activation of PI3K/Akt signaling pathway. Drug Deliv. 2019;26(1):641–9.
38. Duan Y, Zhang Y, Qu C, Yu W, Tana, Shen C. CKLF1 aggravates neointimal hyperplasia by inhibiting apoptosis of vascular smooth muscle cells through PI3K/AKT/NF-kappaB signaling. Biomed

Pharmacother. 2019;117:108986.
39. Gimbrone MA Jr, Garcia-Cardena G. Endothelial Cell Dysfunction and the Pathobiology of Atherosclerosis. Circ Res. 2016;118(4):620–36.
40. Tanabe K, Maeshima Y, Sato Y, Wada J. Antiangiogenic Therapy for Diabetic Nephropathy. Biomed Res Int. 2017;2017:5724069.
41. Coultas L, Chawengsaksophak K, Rossant J. Endothelial cells and VEGF in vascular development. Nature. 2005;438(7070):937–45.

Figures

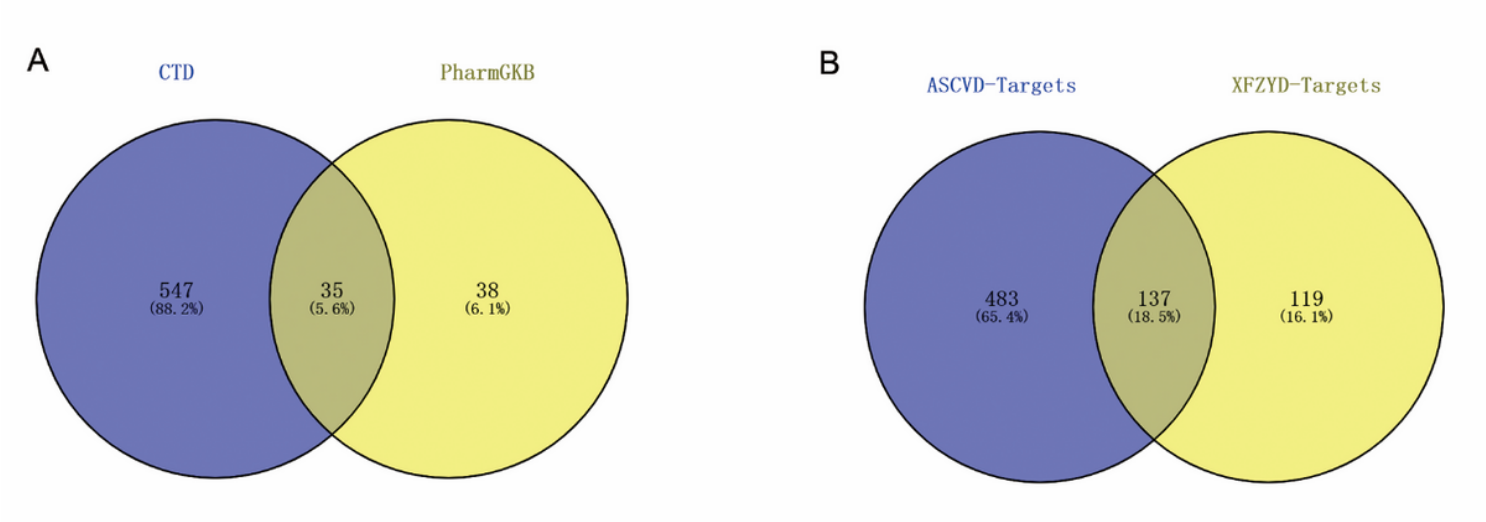

Figure 1

(A)The ASCVD-related targets. (B) The overlapped targets of ASCVD and XFZYD.

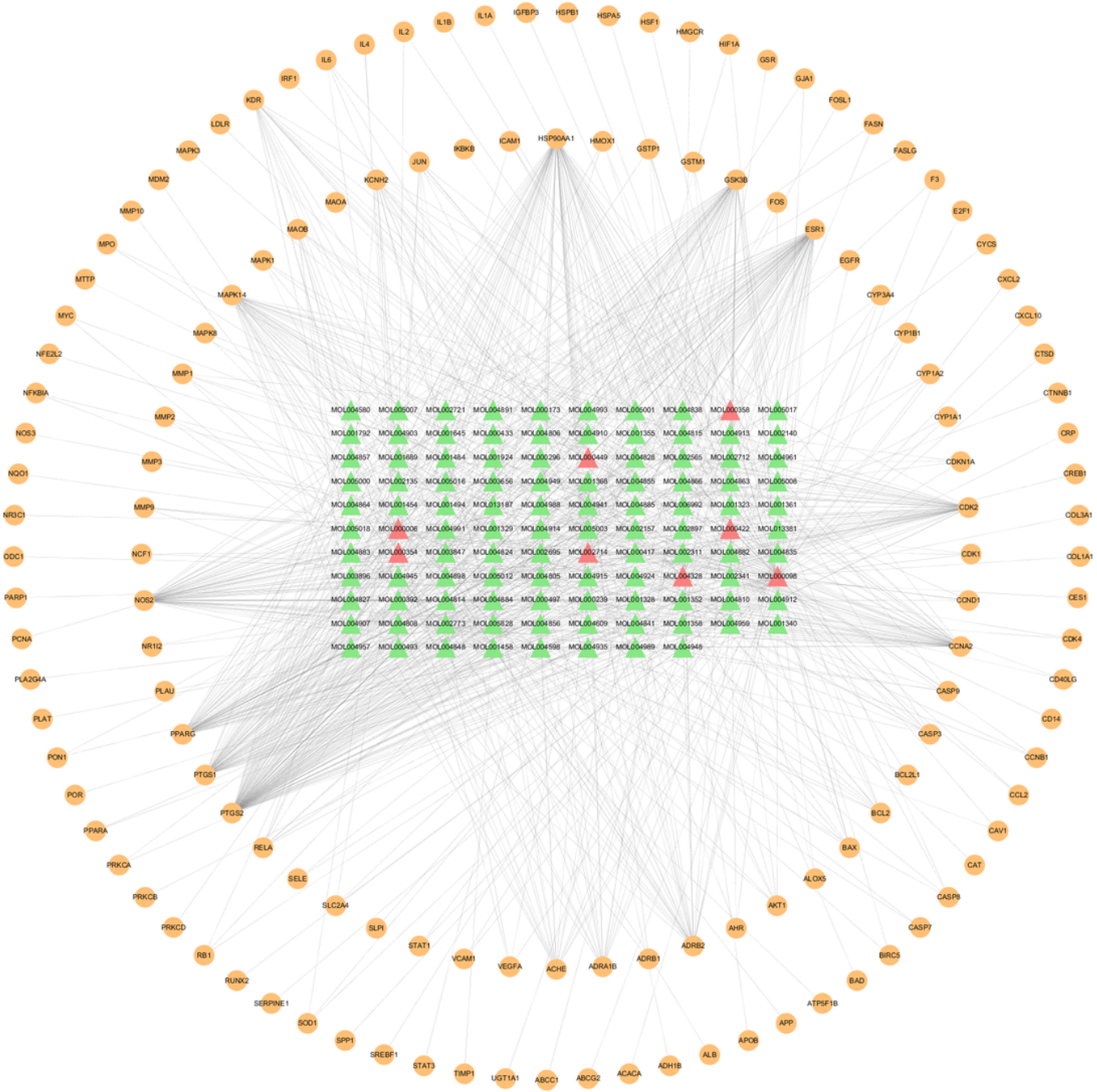

Figure 2

Compounds-targets network of XFZYD in treating ASCVD. Orange ellipse nodes represent potential therapeutic targets, green triangle nodes represent effective compounds, red triangle nodes represent the effective compound originated from multiple herbs.

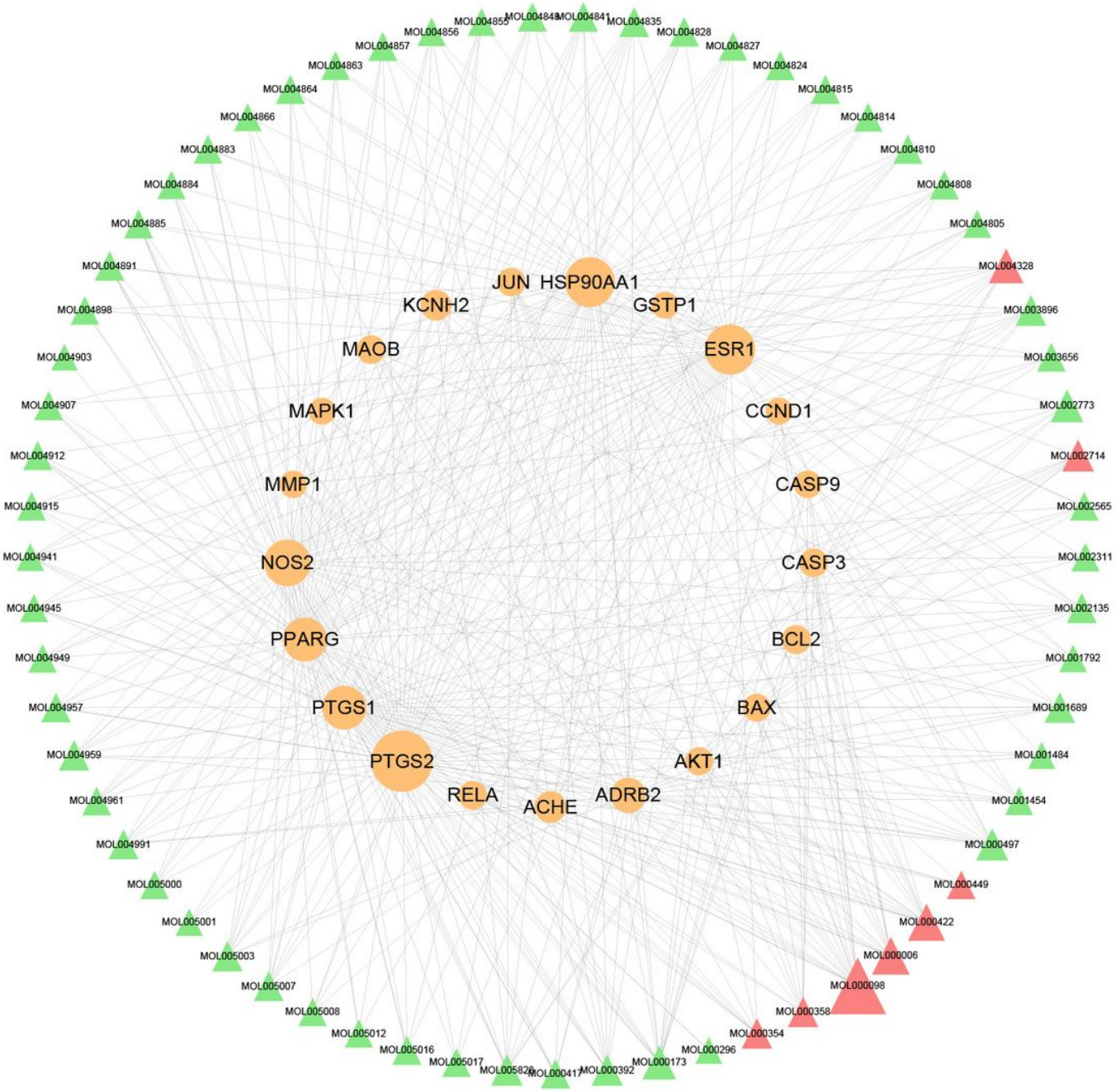

Figure 3

Topological compounds-targets network of XFZYD. Orange ellipse nodes represent potential therapeutic targets, green and red triangle nodes represent effective compounds. The size of node is proportional to the value of the degree centrality by topology analysis.

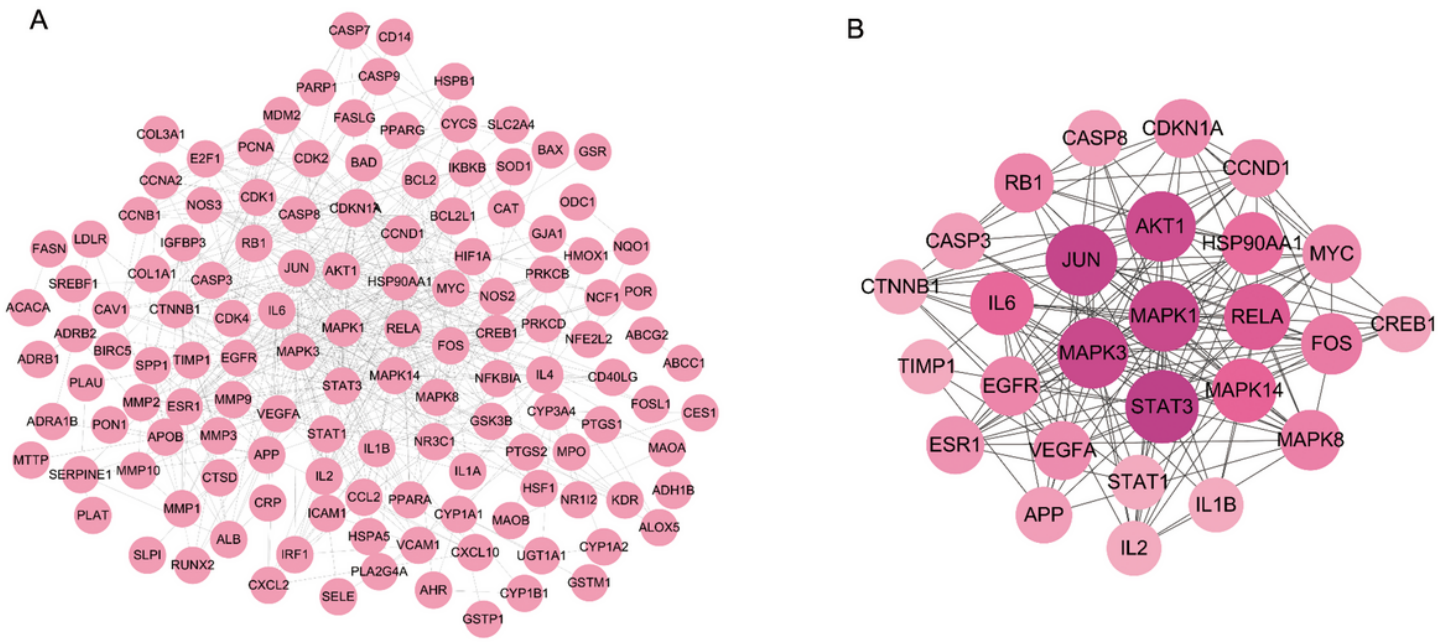

Figure 4

(A) Protein-protein interaction (PPI) network. (B) PPI core network after topology analysis. The size of the circle represents the node degree of the target protein.

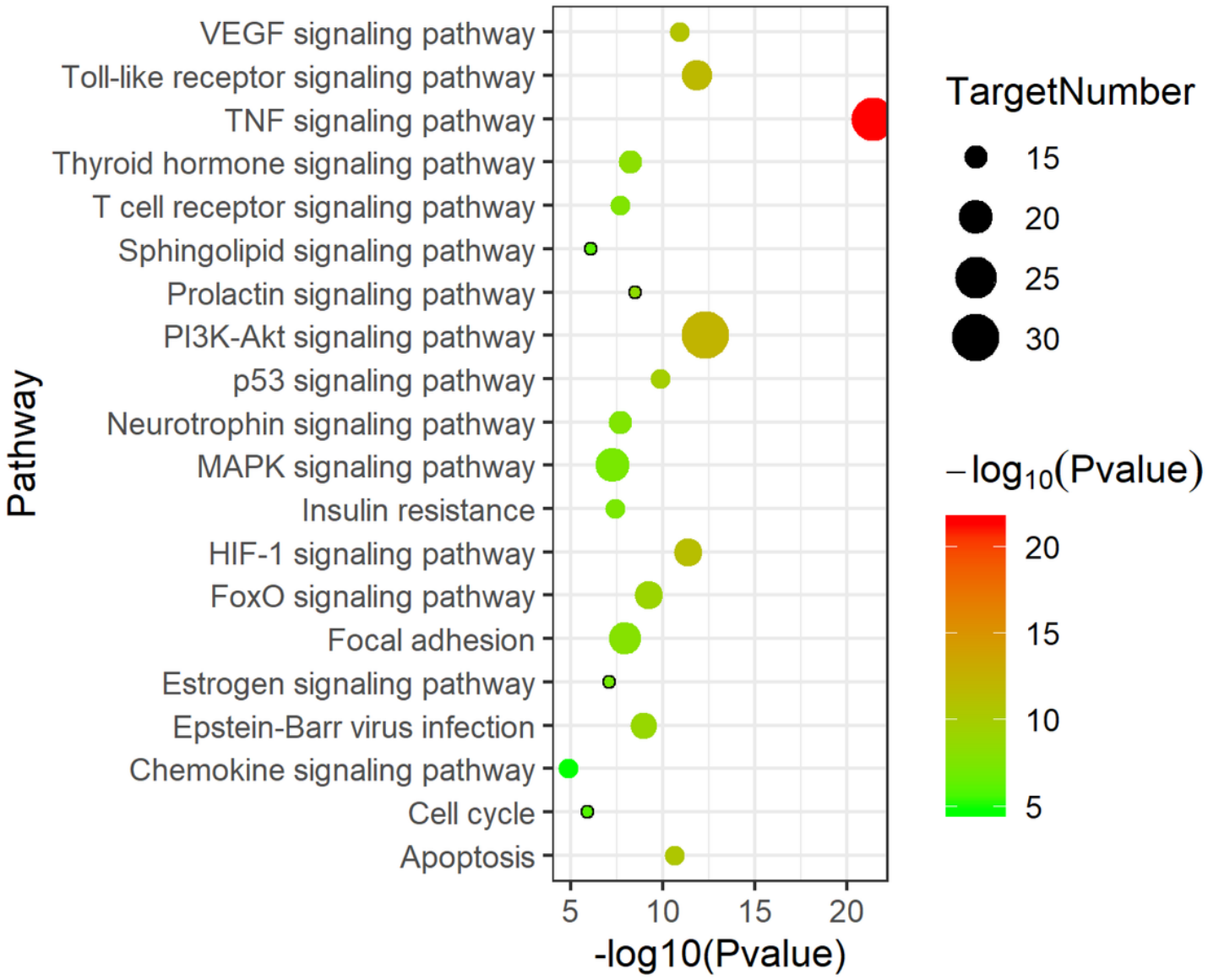

Figure 5

The top 20 KEGG pathway enrichment analyses of 137 target proteins (P value < 0.05).

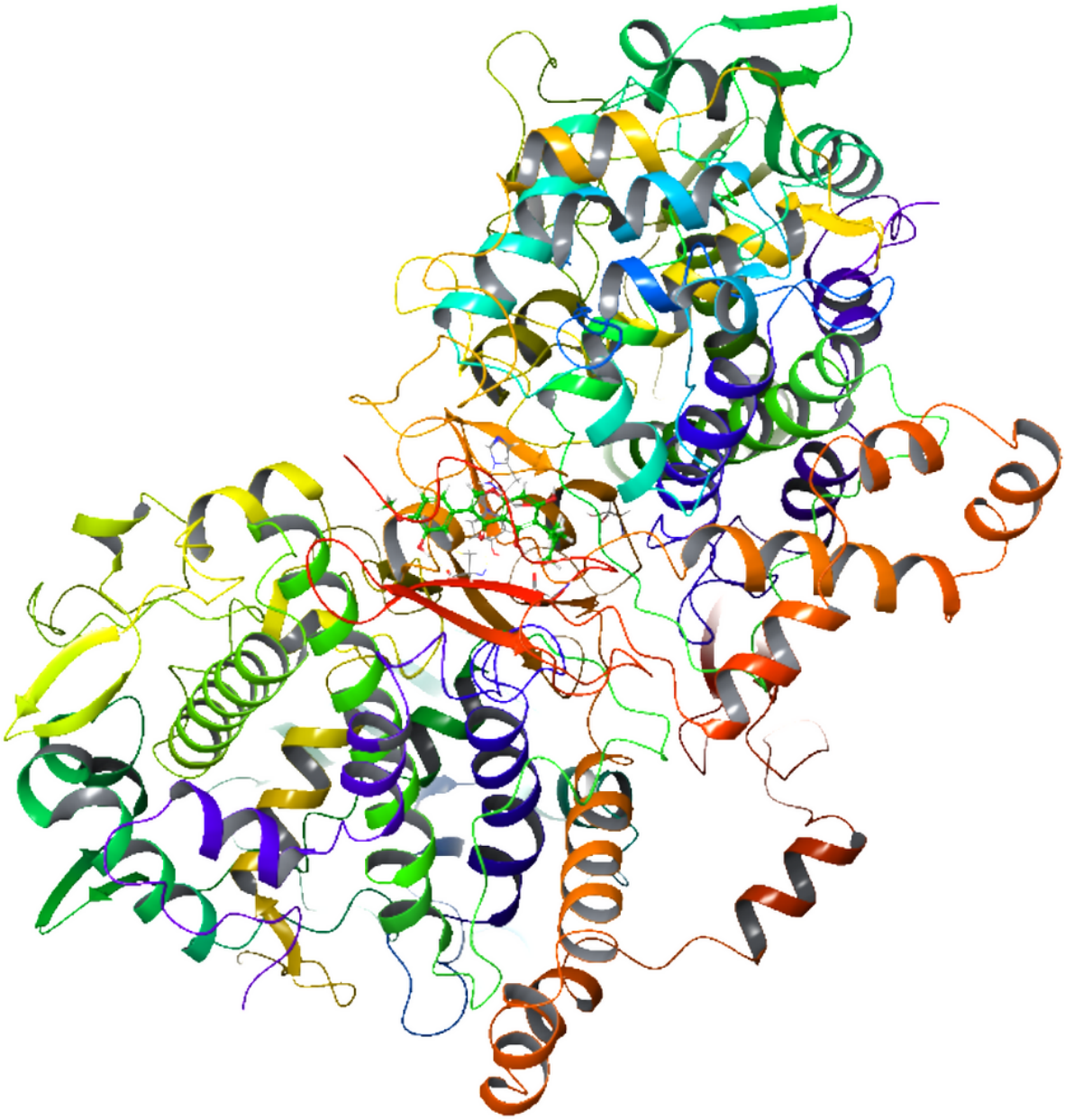

Figure 6

Molecular docking diagram of PTGS2 and Inophyllum E.

Supplementary Files

This is a list of supplementary files associated with this preprint. Click to download.

- Supplementarymaterials.xlsx